CrossMark

Hydrogeochemical assessment of a coastal aquifer using statistical and geospatial techniques: case study of Mombasa North Coast, Kenya

Temitope Ezekiel Idowu[1] · Maurice Nyadawa[2] · Maurice Odondi K'Orowe[3]

Abstract The geochemistry of a coastal aquifer was assessed using statistical and geospatial analysis tools for the pre-monsoon, rainy and post-monsoon seasons. Data were obtained from both the field and laboratory analysis of water samples. Statistical methods such as correlation coefficients, piper plots, factor analysis and mixing index were used to gain insights into the geochemistry, while geospatial tools were used to create contours to understand the spatial distribution of the measured groundwater parameters of the coastal aquifer. The measured groundwater levels ranged from −0.84 to 30.08 m above mean sea level. The Electrical Conductivities and Total Dissolved Solids values were observed to have perfectly correlated with each other. Groundwater salinities were generally high, as over 94% of the water samples tested exceeded the WHO drinking water limit of 750 μS/cm and 500 mg/l, respectively. The groundwater pH was generally slightly alkaline but could be slightly acidic in the rainy season. The Na^+, K^+, Mg^{2+}, Cl^- and SO_4^{2-} were observed to have high impacts on the geochemistry and also had tendencies to form similar trends. EC, TDS and NaCl values above 1000 mg/l in the groundwater were observed to generally skew towards the ocean during the rainy season. The principal process influencing the geochemistry was found to be seawater intrusion, while mineral dissolutions and rainwater percolation play lesser roles. The aquifer predominantly comprises Na–Cl waters of marine origin. The study shows the growing importance and applicability of integrated statistical and geospatial approaches for better understanding of groundwater and geochemistry of aquifers.

Introduction

Over 70% of the world's total freshwater is situated in the sub-surface; however, unregulated and unrestrained abstraction of this groundwater resource can lead to changes in aquifer systems (Kallioras et al. 2013). Coastal aquifers are unique by virtue of their proximity to water bodies where there constantly exists a dynamic interaction between each other (Mondal et al. 2010). Kumar (2006) highlights factors which may affect coastal aquifers as: relative sea level rise; changes in the hydrological regime such as natural recharge, precipitation and evaporation; and coastal zone phenomena such as coastal erosion, shoreline retreat and tidal effect. In cases where deltas and estuaries are present, potential challenges could be backwater effect and seepage of saline surface water into the aquifer (Kumar 2006). Some unpalatable effects of these factors are: salt water intrusion; degradation of coastal ecosystems; decrease in groundwater resources and salt damage of

✉ Temitope Ezekiel Idowu
  lois.temitope@gmail.com

[1] Institute for Basic Sciences Technology and Innovation, Pan African University, Juja, Kenya

[2] Jaramogi Oginga Odinga University of Science and Technology, Bondo, Kenya

[3] Jomo Kenyatta University of Agriculture and Technology, Juja Main Campus, P.O Box 62000-00200, Nairobi, Kiambu, Kenya

🖄 Springer

crops (Kumar 2006). The most noticeable and direct effect is the seawater intrusion. Hence, when the hydrogeological characteristics of a coastal aquifer are being assessed, they are usually done with seawater intrusion in mind.

The importance and usage of groundwater resource have a lot to do with its quality and chemistry, i.e. the concentrations of ions and water quality parameters. Various international and national bodies have set standards for the diverse usage of water (Kenya WASREB 2008; WHO 2011). Groundwater stored in aquifers is affected by both natural and anthropogenic factors. Geological structure, geochemical processes, constituents of precipitation which percolates into the aquifer and rock-water interaction within the aquifer are some of the factors controlling the nature of groundwater found in a place (Sheikhy Narany et al. 2014). The combined effects of these factors dictate the groundwater type; however, the hydrogeochemical processes in the aquifer may also undergo variations in space and time (Belkhiri and Mouni 2013; Sheikhy Narany et al. 2014). Some established methods for investigating the nature of coastal aquifers are: hydrochemical approaches using graphical and multivariate statistical methods (Banoeng-Yakubo et al. 2009; Okiongbo and Douglas 2014; Ziani et al. 2016); numerical modelling (Volker et al. 2002; Sindhu et al. 2012); electrical sounding methods (Olayinka et al. 2004; Yan et al. 2009); ground penetrating radar methods (Beres and Haeni 1991; Gulevich and Volkomirskaya 2015); GIS methods (Balathandayutham et al. 2017; Durgadevagi et al. 2016). Several statistical and graphical methods including: principal component analysis, cluster analysis, fuzzy k-means clustering, Collins bar diagram and Piper plot graphical methods have been examined and compared (Güler et al. 2002). The chemistry of groundwater based on hydrochemical data is expedient for giving baseline information on groundwater types, the study of different chemical activities in the aquifer, identification of the aquifer type, as well as the classification of groundwater based on usage (Mondal et al. 2011a). The recent studies have integrated the application of geographic information systems (GIS) with multivariate statistical approaches for groundwater studies (Somay and Gemici, 2008; Sheikhy Narany et al. 2014). In this study, statistical, graphical and GIS methods were applied in studying the hydrochemistry of the groundwater of the study area. While the hydrochemical analysis provides insights into the nature of groundwater in a study area, GIS is useful in giving a good representation of the spatial distribution of the parameters constituting the groundwater chemistry.

Some previous attempts have been made to study the nature of the aquifers along the coastlines of Eastern Africa. For instance, Mtoni et al. (2012) employed a hydrochemical approach in investigating the interaction between the seawater and the Quaternary aquifer of Dar es Salam and classifying the water types based on the prevalent ions in the water samples. A further groundwater study was conducted in the same region to identify the main hydrogeochemical processes controlling the quality of groundwater as well as the possibility of anthropogenic pollution and seawater intrusion (Mtoni et al. 2013). Another study was conducted on the coastal aquifer of South East Tanzania to detect the groundwater sources and the main factors influencing the groundwater quality with the aid of multivariate statistical analyses (Bakari et al. 2011). Sappa et al. (2015) applied techniques such as principal component analysis (PCA), pattern diagrams and geochemical modelling techniques in identifying the major factors influencing the composition of the groundwater on a seasonal scale and assessing the influence of seasonal changes on groundwater chemistry. All these studies employed the broad technique of hydrochemical analysis. Hence, a good number of groundwater studies have been done on the coastal aquifers of Dar es Salam and its environs, but only a limited number of studies have been carried out on other aquifers along the coast of East Africa. This study, therefore, aims to provide in-depth insights into the groundwater chemistry of the North Coast of Mombasa, Kenya, combining hydrogeochemical and geospatial approaches.

Research area

The study area is located on the North Thrust of the Coast of Mombasa lying between latitudes $3°\ 95''$ and $4°\ 07''$ South of the equator and between longitudes $39°\ 68''$ and $39°\ 72''$ East of the Greenwich meridian (Fig. 1). Mombasa is a major hub of commerce and trade between the East African region (EAC) and the international community. It is also a major tourist destination, attracting both local and international tourists to its beaches, resorts and historical monuments. The North Coast of Mombasa experienced a population increase of over 40% between 1989 and 1999 and over 50% between 1999 and 2009 (GOK 1989, 1999; KNBS 2010), and this trend might likely continue in subsequent decades. The increasing population and booming tourism therefore imply more reliance on the groundwater for livelihoods. Site visits, and Digital Elevation Models (DEM) obtained, indicate that the area is lowly elevated and characterised by a relatively flat topography, with elevations in most parts ranging from 0 to 45 m above mean sea level. The only exceptions are the high elevated hills on the western boundary of the study area. The northern and southern ends of the study area are bounded by creeks, while the coastal edge lies on the Eastern part of the study area (Fig. 1). The geological formation is made up of young sedimentary rocks of Pleistocene epoch, comprising coral limestone along the sea and lagoonal deposits further inland, reaching a thickness of 100 m

Fig. 1 Map of the study area along with the sampling points (*Source:* Idowu et al. 2016)
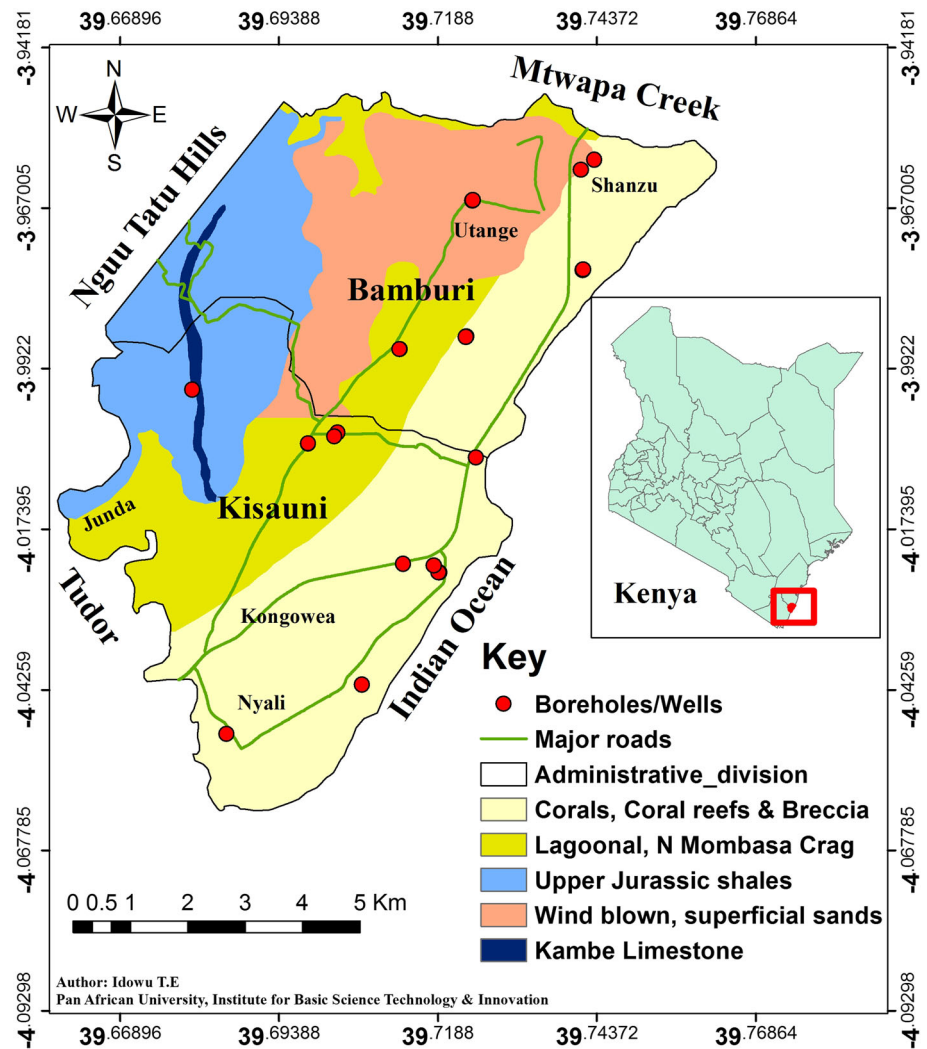
(National Environment Secretariat 1985). The formations are composed mainly of alluvium, wind-blown superficial sands, lagoonal sands, kilindini sands, north Mombasa crag corals and coral breccia which progressively become younger towards the coast (Caswell 2007). The Nguu Tatu hills located on the western boundary of the study area are composed of upper Jurassic shales which are fossiliferous in nature, while the lithology of the area is composed mainly of limestone, sandstone and shale of varying depths (Abuodha 2003; Caswell 2007). The gradients of the continental slope are generally gentle with approximate values of 1:20, and the coral reefs consist mainly of coral limestone, quartz sands, sandstone pebbles, silt and calcareous algae while the Kilindini sands mainly comprise subordinate silts, quartz sands and clays (Abuodha 2003). The general low-lying characteristics aid infiltration and deep percolation of surface runoff, leading to a quick recharge of the aquifer. Hence, the water table is generally shallow and close to the surface (Munga et al. 2006). The climate of the study area is related to the monsoons and the semi-annual passage of the intertropical convergence zone (ITCZ), with the north-eastern monsoon occurring from January to March and the south-eastern monsoon from June to October (National Environment Secretariat 1985). Most rainfall occurs between the monsoon winds, the long rains occurring between March and June while the short rains usually start towards the end of October till December or January. The total annual rainfall is above 1000 mm, with the peak volume of precipitation usually recorded in May (National Environment Secretariat 1985; Climatemps 2015). The coastal aquifer of the Mombasa North Coast is a component of the transboundary coastal sedimentary basin stretching along the coast ends of Kenya and Tanzania (Igrac 2017). The transboundary coastal sedimentary basin, also known as *karoo sedimentary aquifer*, is about 15,000 km^2 and comprises Quaternary and consolidated sedimentary rocks (Barasa et al. 2016; Igrac 2017). The map of the study area, also showing the boreholes/wells from which groundwater data were obtained, is shown in Fig. 1.

Materials and methods

The methodology adopted in this study involves secondary data collection from relevant agencies, field data collection, laboratory tests of water samples, and the statistical and spatial analysis of data. The field data and water samples were obtained for the pre-monsoon, rainy season and post-monsoon on 24 and 25 March, 28 and 29 June and 1 and 2 September 2016, respectively. The data were obtained to cover a half season cycle. The precise locations of bore-holes and sampling wells were captured using a Garmin GPS device. The field data obtained were pH, temperature, EC, TDS and NaCl concentrations. Water samples were then taken for further analysis in the laboratory. The parameters tested in the laboratory include cations: Na^+, K^+, Ca^{2+} Mg^{2+} and anions: Cl^-, HCO_3^- and SO_4^{2-}. Precautions were taken to ensure sample integrity. The basic procedures and water sampling techniques adopted in this study are largely outlined by APHA (1995). The summary of chemical and instrumental techniques used for obtaining the field and laboratory data is highlighted in Table 1.

The exact locations of the sampling boreholes and wells are shown in Fig. 1.

Statistical analysis

The statistical analysis of the data across the three periods entailed correlation matrices to understand the interrelationship amongst the measured parameters and make inferences on their impacts on the groundwater chemistry of the study area (Brown 1998). Piper plots were used to graphically represent the nature of groundwater chemistry in the study area. Principal component analysis (PCA) and mixing index analysis were done to understand the interaction of the aquifer with seawater. The Piper plot is one of the most widely used techniques for visualising the

Table 1 Chemical and instrumental techniques used for water sample analysis

Chemical constituents of groundwater	Techniques used
EC, TDS, pH, NaCl	Portable Eutech waterproof Cyberscan PC 650 and Hanna HI 99,300 devices
HCO_3^-	Volumetric method (Acidimetric neutralisation)
Cl^-	Colorimetric Determination of Chlorine using Mercuric Thiocyanate and Ferric Ion and Spectrophotometer
SO_4^{2-}	Turbidimetric method using spectrophotometer
Na^+, K^+	Flame Emission Spectroscopy
Ca^{2+}, Mg^{2+}	Flame Atomic Absorption Spectroscopy

groundwater chemistry data (Peeters 2013). It comprises the ternary diagrams of major cation and anion compositions, plotted into a central diamond for identifying categories of water samples and the hydrochemical processes influencing the data (Piper 1953).

The "PCA", a method of factor analysis, is a widely applied and probably the oldest and most popular multivariate statistical technique, used to identify trends and obtain the prominent information from a dataset (Abdi and Williams 2010). The PCA analyses the correlations of relationships among variables and try to determine a smaller number of variables that can explain these correlations, i.e. it is a data reduction technique, used to find one or a few number of components that explain all the correlations. The PCA creates a new set of variables having the largest possible variance based on the Eigen values greater than 1 proposed by Kaiser (1960). These new sets of variables are called principal components, and their values are called factor scores. In this study, the parameters: pH, EC, TDS, NaCl, Na^+, K^+, Ca^{2+}, Mg^{2+}, Cl^- and HCO_3^- were analysed from the pre-monsoon, rainy season and post-monsoon datasets. The SO_4^{2-} was only measured at post-monsoon; hence, a separate PCA was done on the post-monsoon data to observe the influence of SO_4^{2-} on the groundwater chemistry. The principal components extracted are orthogonal (uncorrelated) variables generated by varimax rotation involving three major steps: generation of the correlation matrix; factor extraction from the correlation matrix and factor rotation to amplify the relationship between the principal components and the original dataset (Schwartz et al. 2005). The PCA has been widely applied in groundwater studies to not only gain a better understanding of the groundwater chemistry but also infer the presence of pollution like seawater intrusion in coastal aquifers (Al-Ahmadi and Subyani 2010; Mondal et al. 2011a, b; Xuedi et al. 2011; Ravikumar and Somashekar 2015).

Seawater mixing index (SMI) was further applied by Mondal et al. (2011a) in a coastal groundwater to understand the extent of seawater mixing in the aquifer. Seawater mixing is usually higher in the dry season than the rainy season (Schwartz 2006); hence, in this study, the post-monsoon data were analysed based on the principles and equation of SMI (Mondal et al. 2011a). SMI is calculated based on four ions predominant in seawater, i.e. Na^+, Mg^{2+}, Cl^- and SO_4^{2-} with the equation:

$$SMI = a \times \frac{C_{Na}}{T_{Na}} + b \times \frac{C_{Mg}}{T_{Mg}} + c \times \frac{C_{Cl}}{T_{Cl}} + d \times \frac{C_{SO_4}}{T_{SO_4}} \quad (1)$$

where a = 0.31, b = 0.04, c = 0.57 and d = 0.08 representing the relative proportions of concentration Na^+, Mg^{2+}, Cl^- and SO_4^{2-}, respectively, in seawater; C is the observed concentration of the ions in the groundwater

samples (mg/l); T is the calculated regional threshold values of the four ions estimated from cumulative probability curves.

Spatial analysis

Spatial analysis gives a visual dimension and holistic qualitative and quantitative description of the groundwater parameters by showing the spatial distributions. Statistical analysis of groundwater samples only involves the analysis of point data from boreholes/wells; hence, it is limited in application for explaining the spatial distribution of groundwater parameters. The extra advantage spatial analysis has is point data are interpolated geostatistically to form surfaces (Goodchild and Haining 2004), e.g. water table surface, spatial distribution of EC values across the aquifer. Adnan and Iqbal (2014) assessed the groundwater quality of an aquifer by spatially analysing and mapping the groundwater pollutants through the interpolation of water sample data taken from different points to create raster surfaces. A similar study by Durgadevagi et al. (2016) stresses the importance of spatially representing the various parameters constituting the groundwater chemistry. This study involved the spatial interpolation of the EC, TDS and NaCl concentrations in water samples obtained from strategic points in the study area and groundwater level measurements from the boreholes/wells to create contour and spatial variation maps. They were achieved with the aid of geostatistical interpolation tools such as kriging and inverse distance weighted (IDW) in the ArcGIS software. The groundwater levels with respect to the mean sea level were estimated from the static water level measurements using SRTM digital elevation models (DEM) as the benchmarks. These point data were used for generating raster surfaces from which the groundwater table contours were obtained.

Results and discussion

General hydrochemistry

The major parameters were determined for 12 samples in March 2016 and 15 samples each in June and September 2016. Summaries of all the major parameters obtained and tested across the three datasets are presented in Table 2a, b and c. The pH values in the groundwater in March, June and September varied from 6.65 to 8.73 (Table 2a, b and c). However, 40 of the entire 42 samples had pH values above 7, suggesting the groundwater is predominantly slightly alkaline. The only 2 mildly acidic values of 6.65 and 6.98 were observed in the rainy season (Table 2b). The 2 values fall within the WHO pH range for rainwater

(WHO 2011), suggesting the mild acidity may be due to rainfall percolation. All but 3 of the samples fall within the pH range of 6.5–8.5 specified by the Kenya drinking water guidelines implying an acceptability of over 90% of the water samples. Conversely, 24 out of the entire 42 samples fall within the WHO guidelines of 7.5–8.5 implying 57% acceptability. It can be inferred that the groundwater generally has a stable pH irrespective of the seasons.

A close observation of Table 2a, b and c shows that Electrical Conductivities and Total Dissolved Solids levels in groundwater vary considerably across the aquifer. For instance, the EC values ranged from 761.5 to 10,585 μS/cm in March, while TDS values were from 438 to 5281 mg/l within the same time period (Table 2a). This variation in EC and TDS values across the study area was equally observed in June and September. On a seasonal scale, the general trend observed is that EC and TDS values are slightly lower in the aquifer during the rainy season (Table 2b). This may be due to increased groundwater flow associated with high recharge from rainfall during the rainy season. In terms of the allowable standards for drinkable water provided by WHO, the concentration of EC and TDS in over 94% of the water samples taken exceeded the allowable limits of 750 μS/cm and 500 mg/l across the seasons (Table 2a, b and c). However, only slightly >40% exceeded Kenya drinking water limit of 1500 mg/l for TDS contents. NaCl values showed similar observations to those made on EC and TDS values. For instance, a broad range of 660 to 10,569 mg/l NaCl values was observed in March 2016 and also showed similar trends in June and September (Table 3). By assessing the EC (Rai 2004; Mondal et al. 2008), the groundwater samples have been classified into: 1. Fresh (<1500 μS/cm); 2. Brackish (1500–3000 μS/cm); 3. Saline (>3000 μS/cm). The EC classifications for each collection period are represented in percentages and shown in Table 4. The table shows the groundwater is largely brackish/saline with combined percentages of 75, 67 and 73%, respectively, recorded at pre-monsoon, rainy season and post-monsoon. The highest freshwater percentage of 33% was recorded in the rainy season, while the pre-monsoon data accounted for the highest saline water percentage of 42%. Conversely, June reflected the highest freshwater percentage (33%) and the lowest brackish/saline percentage (67%), which suggests salinity is lower in the groundwater during the rainy season. This may be due to the increased groundwater recharge from rainwater infiltration in the rainy season. The boreholes/wells Milele *W5*, Nyali Golf *W6*, SOS W*12* and Sunsweet W*10* are all located along the long stretch of coastline from Nyali on the southern boundary of the study area to Shanzu on the northern end just adjacent to the mtwapa creek (Table 5, Fig. 1). The consistently high values of EC and TDS recorded in them might be due to their proximity of

Table 2 Concentration of the major parameters in the groundwater samples

SN	Sample location	Source type	pH	EC (µS/cm)	TDS (mg/L)	NaCl (mg/L)	HCO_3^- (mg/L)	Cl^- (mg/L)	Mg^{2+} (mg/L)	Ca^{2+} (mg/L)	Na^+ (mg/L)	K^+ (mg/L)
(a) March 2016 (pre-monsoon)												
W1	Braeburn	B	7.38	993	556	982	143.96	166.50	7.31	32.95	125.93	10.54
W2	Cinema	S/W	7.52	1566	839	1450	146.40	212.80	3.93	10.73	136.77	7.40
W3	Krat	B	7.25	2931	1573	2611	119.56	286.40	9.64	26.60	310.73	20.72
W4	M. Hussein	S/W	7.35	1290	754	1185	95.16	197.00	6.84	27.36	102.90	6.74
W5	Milele	B	7.61	10,585	5281	10,569	102.48	366.40	13.30	20.64	735.55	70.24
W6	N golf	B	7.52	3128	1934	3003	109.80	277.00	9.72	19.42	351.45	15.51
W7	Redeem	B	7.63	761.5	438	660	97.60	140.30	0.83	10.13	65.69	2.03
W8	Ruby	B	7.13	1834	1143	1743	173.24	257.80	6.93	7.39	219.80	6.99
W9	Sos	S/W	7.41	4427	2295	4406	87.84	348.60	11.47	28.42	412.41	28.49
W10	Sunsweet	B	7.2	4647	2330	4320	87.84	336.20	10.91	24.44	406.28	18.65
W11	Utange	B	7.82	1966	1028	1824	129.32	266.00	7.08	6.93	271.60	14.18
W12	Vikwatani	S/W	7.64	6711	2915	6832	139.08	379.60	13.10	32.84	482.62	13.19
Drinking water standard (WHO 2011)			7.5–8.5	750	500		300	200	30	75	200	100
Kenya Drinking Water Standards (Kenya 2008)			6.5–8.5		1500			250	100	250	200	200
(b) June 2016 (rainy season)												
W1	Braeburn	B	7.95	1150	596	980	108.82	67.92	1.11	2.49	108.48	4.10
W2	Cinema	S/W	6.65	1626	846	1573	68.32	81.99	1.14	3.02	180.12	8.64
W3	Krat	B	7.94	462	240	370	39.04	43.79	1.05	0.81	39.23	8.73
W4	M. Hussein	S/W	7.53	1260	656	1143	53.68	62.82	1.08	1.86	47.12	3.27
W5	Milele	B	8.24	9196	4588	9452	73.20	149.85	1.33	2.34	726.46	61.89
W6	N golf	B	6.98	3804	1974	3825	87.84	25.02	1.23	3.43	323.00	14.10
W7	Redeem	B	7.97	762	425	642	73.20	10.38	0.97	2.64	49.51	1.37
W8	Ruby1	B	8.70	550	285	443	48.80	50.51	1.06	0.95	64.25	9.97
W9	Ruby2	B	8.33	1861	968	1719	126.88	87.71	1.14	1.57	216.94	5.50
W10	Shimo high	S/W	7.06	4038	2020	4093	97.60	102.64	1.13	5.02	172.39	7.40
W11	Shimo qtrs	B	7.35	1944	1009	1820	92.72	104.59	1.13	4.04	169.76	6.16

Table 2 continued

SN	Sample location	Source type	pH	EC (µS/cm)	TDS (mg/L)	NaCl (mg/L)	HCO$_3^-$ (mg/L)	Cl$^-$ (mg/L)	Mg^{2+} (mg/L)	Ca^{2+} (mg/L)	Na$^+$ (mg/L)	K$^+$ (mg/L)
W12	Sos1	S/W	7.46	4056	2073	3924	45.56	100.92	1.21	2.09	323.48	17.99
W13	Sos2	S/W	7.41	3122	1624	3109	97.60	123.05	1.20	17.71	285.95	11.70
W14	Sunsweet	B	7.22	4036	2074	3909	53.68	80.52	1.23	2.95	301.64	9.80
W15	Utange	B	8.61	1916	996	1793	156.16	92.91	1.14	1.55	224.11	7.82
Drinking water standard (WHO 2011)			7.5–8.5	750	500		300	200	30	75	200	100
Kenya Drinking Water Standards (Kenya 2008)			6.5–8.5		1500			250	100	250	200	

(c) *September 2016 (post-monsoon)*

SN	Sample location	Source type	pH	EC (µS/cm)	TDS (mg/L)	NaCl (mg/L)	HCO$_3^-$ (mg/L)	Cl$^-$ (mg/L)	Mg^{2+} (mg/L)	Ca^{2+} (mg/L)	Na$^+$ (mg/L)	K$^+$ (mg/L)	SO$_4$ (mg/L)
W1	Braeburn	B	7.72	1180	610	1003	140.54	135.80	1.49	10.89	171.35	6.15	95.35
W2	Cinema	S/W	7.57	1603	835	1451	154.60	145.50	1.51	14.79	184.70	8.10	98.31
W3	Krat	B	8.73	480	250	376	108.92	132.10	1.08	1.14	47.44	8.87	78.91
W4	M. Hussein	S/W	7.46	1314	687	1140	125.32	134.50	1.39	13.5	73.70	3.94	150.50
W5	Milele	B	7.90	9516	4748	9781	78.29	279.91	1.74	0.67	729.10	65.77	257.19
W6	N golf	B	7.51	3805	1977	3725	108.92	137.60	1.64	4.32	298.40	8.00	221.46
W7	Redeem	B	7.68	713	371	579	89.01	117.60	0.85	13.19	70.70	1.74	89.54
W8	Ruby2	B	7.8	1896	986	1705	189.15	123.60	1.48	5.71	215.70	3.09	134.49
W9	Shimo high	B	7.88	1586	824	1402	107.75	139.00	1.44	18.44	101.80	2.67	100.95
W10	Shimo qtrs	S/W	7.96	1985	1033	1815	105.41	140.20	1.52	14.56	157.40	4.37	122.95
W11	Sos1	B	8.00	4188	2140	4052	73.79	151.30	1.60	2.89	462.70	22.90	158.56
W12	Sos2	S/W	7.98	3490	1812	3327	106.58	149.30	1.63	4.07	440.60	21.40	220.47
W13	Sunsweet	S/W	7.57	4157	2135	4025	92.52	137.46	1.66	3.73	179.96	8.70	170.46
W14	Utange	B	7.48	1910	992	1726	156.36	122.46	1.48	2.93	203.60	6.30	143.41
W15	Vikwatani	S/W	7.92	6184	3143	6183	165.14	134.96	1.74	2.98	375.67	6.58	328.92
Drinking water standard (WHO 2011)			7.5–8.5	750	500	200	300	200	30	75	200	100	200
Kenya drinking water standards			6.5–8.5		1500	400		250	100	250	200		400

pH log10H$^+$, *TDS* total dissolved solids in mg/l, *EC* electrical conductivity in µS/cm, all other ions are in mg/l, *B* boreholes, *S/W* Shallow wells

Table 3 Statistical analysis of the parameters across the three periods

Parameters	Unit	Min	Max	Mean
March				
pH	–	7.13	7.82	7.46
EC	(μS/cm)	761.5	10,585	3403.21
TDS	(mg/L)	438	5281	1676
NaCl	(mg/L)	659.8	10,569	3324.7
HCO_3^-	(mg/L)	87.84	173.24	119.36
Cl^-	(mg/L)	140.30	379.60	269.55
Mg^{2+}	(mg/L)	0.83	13.30	8.42
Ca^{2+}	(mg/L)	6.93	32.95	20.65
Na^+	(mg/L)	65.69	735.55	301.81
K^+	(mg/L)	2.03	70.24	17.89
June				
pH	–	6.65	8.70	7.69
EC	(μS/cm)	462	9196	2652
TDS	(mg/L)	240	4588	1676
NaCl	(mg/L)	370	9452	2669
HCO_3^-	(mg/L)	39.04	156.16	88.16
Cl^-	(mg/L)	10.38	149.85	75.52
Mg^{2+}	(mg/L)	0.97	1.33	1.14
Ca^{2+}	(mg/L)	0.81	17.71	3.50
Na^+	(mg/L)	39.23	726.46	215.50
K^+	(mg/L)	1.37	61.89	11.90
September				
pH	–	7.46	8.73	7.81
EC	(μS/cm)	480	9516	2934
TDS	(mg/L)	250	4748	1503
NaCl	(mg/L)	376	9781	2867
HCO_3^-	(mg/L)	51.53	189.15	118.37
$Cl-$	(mg/L)	108.80	154.30	139.49
SO_4^{2-}	(mg/L)	78.91	328.92	158.10
Mg^{2+}	(mg/L)	0.85	1.74	1.48
Ca^{2+}	(mg/L)	0.19	18.44	7.56
Na^+	(mg/L)	47.44	729.10	247.52
K^+	(mg/L)	1.74	65.77	11.91

Table 4 Fresh, Brackish and Saline water types in the groundwater in percentages

Groundwater type	March 2016 (%)	June 2016 (%)	September 2016
Fresh	25	33	27
Brackish	33	27	33
Saline	42	40	40

<500 m to the Indian Ocean. Also, Vikwatani *W16* close to the Nguu Tatu hills on the western boundary was observed to consistently contain high EC and TDS values (Table 2). The relatively higher groundwater table of

>25 m above mean sea level (Table 5) implies that the high EC and TDS values may not only be due to seawater mixing but also other complex geological processes. However, the spatial distributions of the EC, TDS and NaCl values derived from spatial analysis give more veritable representation of the values and spread of these parameters in the groundwater.

Of the four cations tested, Na^+ had the highest concentration over the study period showing values as high as 736 mg/l in a sample (Table 3). However, the Na^+ concentrations were observed to be generally lower in June (Table 2a, b and c). Over 50% of the water samples taken from the three periods exceeded the allowable limit of 200 mg/l for Na^+ content specified by both WHO and Kenya drinking water guidelines. However, Ca^{2+}, K^+ and Mg^{2+} concentrations in all the water samples were within the allowable limits specified by both regulatory bodies (Table 2a, b and c). The Mg^{2+} and Ca^{2+} exist in much smaller quantities in comparison with Na^+ and K^+. This observed difference between Mg^{2+} & Ca^{2+} and Na^+ and K^+ concentrations is more evident in the samples taken in June (Table 2b) where the concentrations of ions were generally lower. The lower concentrations imply that the groundwater quality tends to be higher in the rainy season.

The anions exhibited varying trends across the aquifer and over the three datasets. The concentrations of chloride ions in groundwater ranged from 140.30–379.60 mg/l in March (pre-monsoon), and dropped to a range of 10.38–149.85 mg/l in June and 108.80–154.30 mg/l in September. Conversely, HCO_3^- concentration ranges were 87.84–173.24, 39.04–156.16 and 51.53–189.15 mg/l in the same period (Table 3). This implies the variation of chloride ions across the aquifer reduced from the dry (pre-monsoon) to the wet season, while the reverse was the case with bicarbonate concentrations. The SO_4^{2-} ions tested in September varied from 78.91 to 328.92 mg/l in the water samples. The chloride concentrations of 75% of the water samples taken in March exceeded WHO's allowable limit for drinking water (WHO 2011), while over 50% exceeded the Kenya drinking water guidelines (Kenya WASREB 2008). In the case of SO_4^{2-}, 4 out of 15 samples exceeded 200 mg/l limit specified by WHO's drinking water limit while all the samples satisfied the 400 mg/l Kenya drinking water guidelines limit (Table 2c). Overall, the relatively high values of EC, NaCl, Na^+ and Cl^- across the three periods of data collection (Table 2) suggest that the groundwater in a large portion of the aquifer is unsuitable for direct drinking purposes but may be useful for general domestic use.

Correlation matrices

The use of correlation matrices to assess the relationships amongst groundwater quality parameters is not only

Table 5 The sampled boreholes/wells showing the geographic coordinates and the water tables above mean sea level

SN	Sample location	Longitude	Latitude	Depth of well (m)	MSL of MP (m)	March		June		September	
						WLM	MSL of GW (m)	WLM (m)	MSL of GW (m)	WLM (m)	MSL of GW (m)
W1	Braeburn	580281.0326	9559250.6848	15.5	17	14.10	2.90	13.17	3.83	13.23	3.77
W2	Cinema	576106.3909	9552365.9589	22	19	18.10	0.90	17.94	1.06	17.80	1.20
W3	Krat	579181.2187	9555320.1432	27	19	14.00	5.00	14.50	4.50	14.52	4.48
W4	M. Hussein	577531.7055	9557403.1077	28	30	24.95	5.05	24.51	5.49	24.61	5.39
W5	Milele	580455.1451	9557154.2796	12.5	11	10.36	0.64	9.94	1.06	10.19	0.81
W6	N golf	578466.5947	9553221.3129	10	18	9.10	8.90	8.96	9.04	8.90	9.10
W7	Redeem	580398.9022	9561622.8615	30	24	21.65	2.35	20.24	3.76	21.07	2.93
W8	Ruby1	578051.0775	9557591.8047	30	30	24.50	5.50	28.70	1.30	–	–
W9	Ruby2	577986.0766	9557524.2075	29	29	–	–	25.94	3.06	26.14	2.86
W10	Shimo high	582518.5623	9562327.3646	15	18	–	–	14.95	4.45	12.16	5.84
W11	Shimo qtrs	582283.2633	9562151.0353	26	17	–	–	13.55	2.05	14.15	2.85
W12	Sos1	579799.9737	9555168.7077	9.15	13	8.61	4.39	7.40	5.60	8.37	4.63
W13	Sos2	579715.5969	9555285.5167	10	11	–	–	7.50	3.50	7.46	3.54
W14	Sunsweet	582320.1225	9560416.5563	15	14	12.46	1.54	14.95	–0.95	14.84	–0.84
W15	Utange	579126.6152	9559040.4411	26	25	21.65	3.35	10.46	10.46	12.40	12.60
W16	Vikwatani	575516.7016	9558338.7809	20	43	16.11	29.89	16.14	26.86	12.92	30.08

W wells, *WLM* water level measurement, *MSL* mean sea level, *MP* measuring point, *GW* groundwater

MSL of GW = MSL of MP–WLM. projected coordinate system: WGS_1984_utm_zone_37s

beneficial in evaluating the overall quality of groundwater but also gives insights on pollution for effective water quality management (Jothivenkatachalam et al. 2010). Correlation matrices were developed for each of the parameters tested in the groundwater in the study area. High correlation coefficients "r" (i.e. values close to −1 and 1) implies strong relationships between the variables of one parameter and the other (Ratner 2009). Strong positive correlations are indicators of the significance of the parameter in the groundwater chemistry of the study area and their tendency to follow a similar trend (Adams et al. 2001; Mondal et al. 2011b). The correlation coefficients *r* for the various parameters tested are presented for the pre-monsoon, rainy and post-monsoon seasons and highlighted in Table 6.

The correlation matrices for the three datasets were observed to all follow a similar trend. EC and TDS for the three periods had correlation coefficient values 0.99, 1.00 and 1.00, respectively, implying an absolute direct linear relationship (Table 6). The EC and TDS were also observed to consistently have strong correlations with Na^+, Mg^{2+}, Cl^- and K^+ over the three datasets (Table 6). It can be inferred that these parameters play significant roles in defining the groundwater geochemistry of the study area. Mondal et al. (2011b) noted that high correlation of

groundwater parameters is suggestive of the parameters/ions controlling the chemistry of the groundwater. Cl^- showed a strong positive relationship with Na^+ and K^+ across the three datasets signifying that these three parameters heavily influence the EC and TDS contents of the groundwater. It is noteworthy that Na^+ had a strong positive relationship with Mg^{2+} and K^+ across the three periods, while Mg^{2+} had a strong positive relationship with K^+ in both March and June. Na^+, Mg^{2+} and K^+ are known to exist in much larger quantities in seawater in comparison with continental freshwater (Moujabber et al. 2006), thereby implying the groundwater salinity may be due to the influence of the seawater body in proximity to the groundwater aquifer. Conversely, HCO_3^- and Ca^{2+} had no consistent relationship with other parameters/ions across the three time periods. This lack of consistent relationship was also observed in the pH values. The pH values had no correlation with the other parameters in the groundwater and followed no consistent trend. The water samples taken in September were tested for SO_4^{2-} concentration (Table 2c), and it was observed that SO_4^{2-} strongly correlates with EC, TDS, Na^+ and Mg^{2+} which have been identified to have strong positive correlations amongst themselves.

Hence, the main parameters controlling the groundwater chemistry are EC, TDS, Cl^-, Na^+, Mg^{2+}, K^+, and to some

Table 6 Correlation coefficients for the groundwater parameters for the coastal aquifer of the North Coast of Mombasa (Moujabber et al. 2006)

Parameters	pH	EC	TDS	Cl	HCO_3	Na	Mg	Ca	K
March (pre-monsoon)									
pH	1.00								
EC	0.19	1.00							
TDS	0.13	0.99	1.00						
Cl	0.02	0.84	0.89	1.00					
HCO_3	−0.09	−0.26	−0.29	−0.18	1.00				
Na	0.16	0.97	0.99	0.91	−0.25	1.00			
Mg	−0.08	0.81	0.86	0.91	−0.2	0.88	1.00		
Ca	−0.24	0.31	0.32	0.32	−0.3	0.27	0.60	1.00	
K	0.16	0.87	0.85	0.63	−0.3	0.87	0.66	0.18	1.00
June (rainy season)									
pH	1.00								
EC	−0.13	1.00							
TDS	−0.12	1	1.00						
Cl	0.05	0.56	0.56	1.00					
HCO_3	0.13	0.13	0.12	0.25	1.00				
Na	−0.02	0.96	0.96	0.58	0.22	1.00			
Mg	−0.22	0.86	0.86	0.55	0.30	0.91	1.00		
Ca	−0.32	0.14	0.14	0.36	0.14	0.15	0.23	1.00	
K	0.16	0.88	0.89	0.56	−0.13	0.90	0.73	−0.01	1.00

Parameters	pH	EC	TDS	Cl	HCO_3	Na	Mg	Ca	K	SO_4^{2-}
September (post-monsoon)										
pH	1.00									
EC	−0.07	1.00								
TDS	−0.08	1	1.00							
Cl	0.06	0.80	0.79	1.00						
HCO_3	−0.21	−0.39	−0.39	−0.38	1.00					
Na	−0.02	0.90	0.91	0.79	−0.38	1.00				
Mg	−0.25	0.70	0.71	0.42	0.03	0.67	1.00			
Ca	−0.55	−0.57	−0.57	−0.33	0.14	−0.59	−0.34	1.00		
K	0.18	0.81	0.80	0.96	−0.60	0.87	0.41	−0.50	1.00	
SO_4^{2-}	−0.21	0.84	0.84	0.42	−0.06	0.78	0.71	−0.56	0.46	1.00

degree SO_4^{2-} while changes in Ca^{2+}, HCO_3^- and pH have minimal impacts on the geochemistry of the study area.

Piper plots

Piper plot is one of the most widely applied methods for characterising groundwater (Karmegam et al. 2011; Musa et al. 2014), and it categorises ground water as any of the following: Ca-SO_4 waters, Na-SO_4 waters, Ca–Cl waters, Na–Cl waters, Na-HCO_3 waters or Ca-HCO_3 waters (Adams et al. 2001). Ca-SO_4 waters are typical of gypsum groundwaters and mine drainages; Ca-HCO_3 waters are indicative of shallow fresh groundwater; Na–Cl waters are indicative of marine and deep ancient groundwaters, while Na-HCO_3 waters typify deeper groundwater influenced by ion exchange (Piper 1953). The piper plot was obtained for post-monsoon data for two reasons: 1. Seawater influence is higher in the groundwater during the dry season; 2. The SO_4^{2-} measurements were only available for the post-monsoon data of this study (Fig. 2). The concentrations of the cations (Na, K, Mg, Ca) and anions (Cl, HCO_3, SO_4) were all normalised and plotted into the piper plot as shown in Fig. 3.

The groundwater samples fall within the "Na–Cl waters" quadrant in the diamond (Fig. 2) which implies the groundwater is of the marine and deep ancient type (Piper
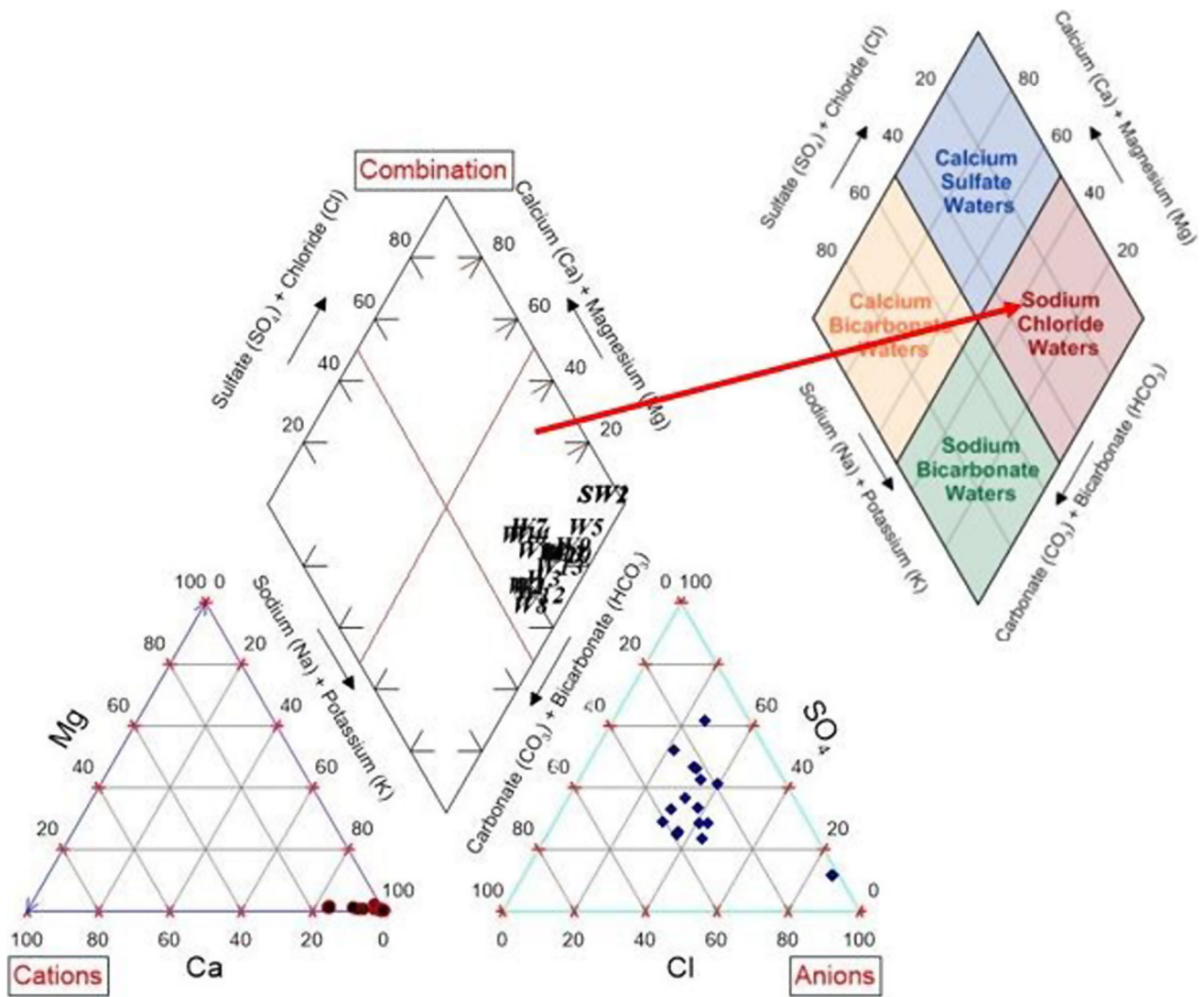
Fig. 2 *Piper plot* for the water samples taken in the study area
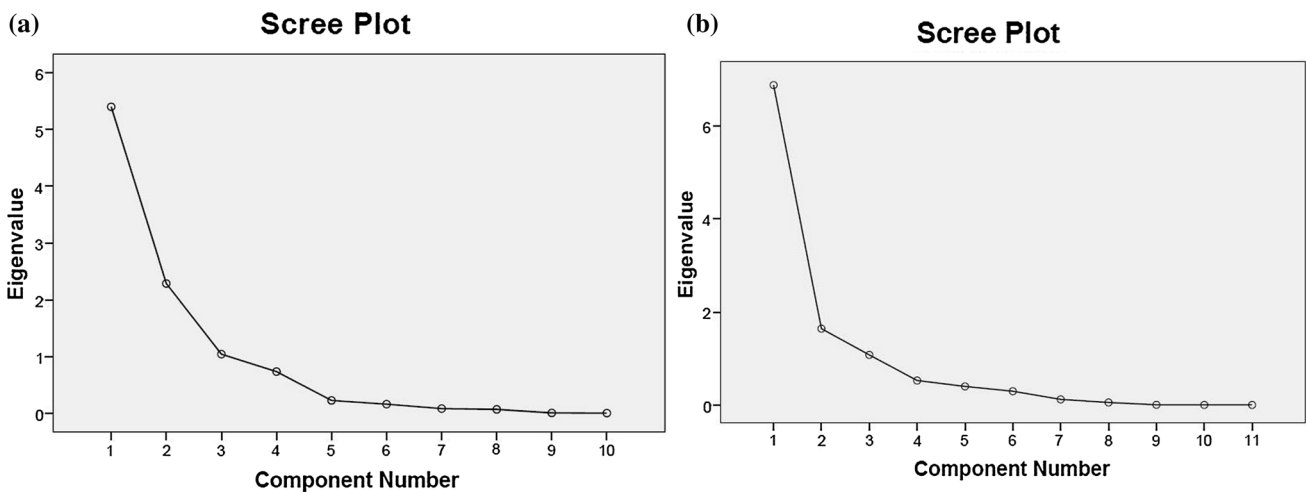
Fig. 3 *Scree plots* showing the components against the Eigen values **a** combined dataset **b** September dataset

1953). This suggests the presence of salinization (Adams et al. 2001) due to the dynamic movement of the seawater interface over geological time periods. The study area stretches from the seafront to about 7 km inland while it is bounded to the north and south by creeks implying a constant interaction between the aquifer and the adjourning saltwater bodies for several thousands of years. This explains why the water samples all point towards being of marine origin.

Principal components analysis

The variables pH, EC, TDS, NaCl, Na$^+$, K$^+$, Ca^{2+}, Mg^{2+}, Cl$^-$ and HCO$_3^-$ were analysed to obtain the principal components for the entire 42 samples obtained. Furthermore, a separate factor analysis was done for the post-monsoon data to account for the SO$_4^{2-}$ variable present. The total number of components in factor analysis is equal to the number of variables in the dataset. This is observed in the scree plots showing 10 and 11 components, respectively, in a and b (Fig. 3). Varimax orthogonal rotation with Kaiser normalisation was used to extract the principal components. The scree plots show that three components (factors) have Eigen values >1 in both analysis, and these are the principal components extracted as shown in Table 7. The three principal components (factors) obtained accounted for a cumulative 87.33% of the variance for both factor analysis, i.e. the combined dataset and post-monsoon dataset (Table 7).

Three principal components imply there are three distinct processes contributing to the groundwater chemistry.

For the combined dataset, component I with the highest variance of 54.03% has EC, TDS, NaCl, Na$^+$ and K$^+$ with high positive loadings >0.9. High values of EC and TDS could be as a result of seawater mixing but also anthropogenic influences; however, NaCl, Na$^+$, K$^+$ are highly indicative of seawater intrusion. Hence, the principal component I suggests the influence of seawater intrusion. Component II has Mg^{2+}, Ca^{2+} and Cl$^-$ with high positive loading >0.8. These ions in groundwater are usually as a result of a wide range of complex natural processes. The pH and HCO$_3^-$ parameters have high positive loadings >0.7 in Component III. The pH could be as a result of changes in mineral compositions in groundwater as well as the mixing of rainwater with the groundwater through deep percolation. HCO$_3^-$ in groundwater is usually as a result of dissolution of carbonate minerals in the aquifer. Since the lithology of the aquifer comprises mostly limestone, sandstone and shale, HCO$_3^-$ concentrations in the groundwater might be as a result of the dissolution of the minerals in the aquifer. Hence, the main contributor to the groundwater chemistry is seawater interaction (component I), and to lesser extents: complex natural processes, mineral dissolutions in the aquifer formation and rainwater percolation. The factor analysis for the post-monsoon dataset largely confirms the identified processes.

Component I of post-monsoon data set has additional parameters Mg^{2+}, Cl$^-$ and SO$_4^{2-}$ with high positive loadings >0.5 and Ca^{2+} with a high negative loading >−0.6. The Mg^{2+}, Cl$^-$ and SO$_4^{2-}$ are predominant in seawater, while Ca^{2+} concentrations are relatively higher in continental freshwater. This further shows that seawater

Table 7 Varimax rotated Principal component matrices and the variables of the groundwater samples

Variables	Combined dataset			Variables	Post-monsoon dataset		
	Component I	Component II	Component III		Component I	Component II	Component III
pH	0.085	−0.467	0.707	pH	−0.157	0.200	0.885
EC	0.973	0.131	−0.048	EC	0.913	0.371	0.059
TDS	0.974	0.131	−0.057	TDS	0.918	0.362	0.056
NaCl	0.973	0.121	−0.049	NaCl	0.908	0.381	0.065
HCO$_3$	−0.181	0.405	0.720	HCO$_3$	0.066	−0.842	−0.113
Cl	0.460	0.818	0.135	Cl	0.588	0.729	0.031
Mg	0.291	0.888	0.000	Mg	0.844	−0.079	−0.208
Ca	−0.031	0.906	−0.060	Ca	−0.611	0.047	−0.651
Na	0.952	0.180	0.033	Na	0.851	0.402	0.124
K	0.923	0.075	−0.031	K	0.620	0.709	0.175
–	–	–	–	SO$_4$	0.916	−0.067	0.059
Initial Eigen values of variance in (%)	54.03	22.88	10.42	–	62.59	14.94	9.80
Cumulative % of variance	54.03	76.91	87.33	–	62.59	77.52	87.33
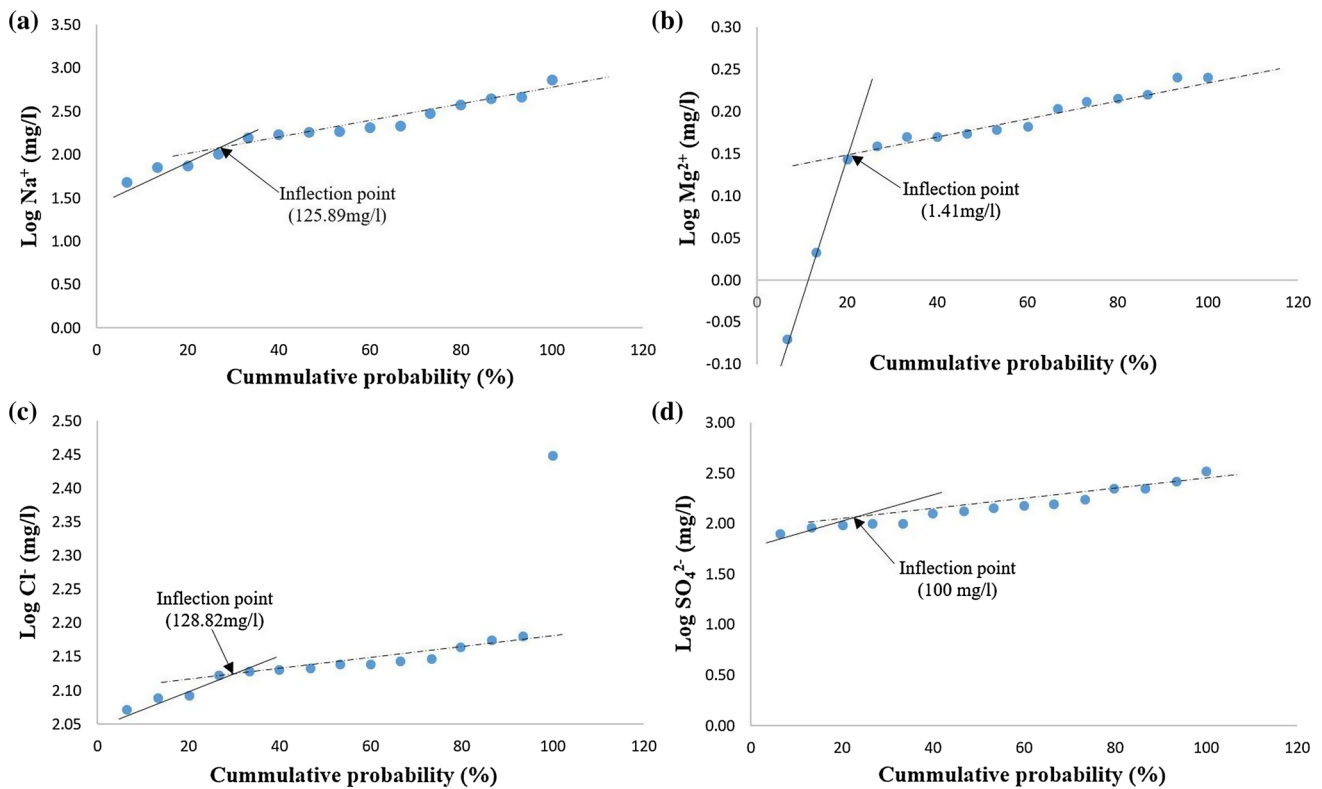
Fig. 4 Plots of cumulative probability versus log of concentrations a. Na^+, b. Mg^{2+}, c. Cl^-, d. SO_4^{2-} in the groundwater

interaction plays the major influence on the groundwater chemistry.

Seawater mixing index

Based on Eq. 4, the seawater mixing index was calculated for the post-monsoon dataset using the concentrations and threshold values of Na^+, Mg^{2+}, Cl^- and SO_4^{2-} known to be high indicators of the presence of seawater intrusion. The regional threshold values (T) of the four chosen parameters were derived from the inflection points of the cumulative probability plots against the log of the concentration of the parameters (Fig. 4).

The approximate regional threshold concentrations estimated are 125.89, 1.41, 128.82 and 100 mg/l for Na^+, Mg^{2+}, Cl^- and SO_4^{2-}, respectively. SMI values of all the groundwater samples varied from 0.79 to 3.30. The results of a similar SMI study by Mondal et al. (2011a) showed SMI values of a range 1.98–22.40 for the Na–Cl water types identified in the study area. In contrast, the extent of seawater mixing in this study shows a much lower range. This implies the impact of the seawater intrusion observed in the coastal aquifer of Tamil Nadu, India, is much higher than that observed in the North Coast of Mombasa Kenya in this study.

Spatial analysis

The groundwater levels above or below the mean sea level were estimated from static water level measurements from the boreholes/wells. Since the topography of any area on the earth's surface is uneven, the digital elevation model for the study area was used to estimate the actual water levels with respect to the mean sea level as shown in Table 5. At pre-monsoon, the groundwater level measurements varied from 0.90–29.89 m above mean sea level (msl) while −0.95 to 26.86 m and −0.84 to 30.08 above msl were observed during the rainy season and post-monsoon, respectively (Table 5). This implies the groundwater levels could be slightly below mean sea level in some parts of the study area depending on the season and abstraction rate. However, these are point measurements which may not be fully representative of all parts of the aquifer. Hence, the spatial analysis is required to produce raster surfaces and contours.

The point groundwater measurements were interpolated to produce the *rasters* of the water table. The groundwater table contours obtained from the groundwater table rasters showed little variation across the seasons, varying from 0 to 27 m above mean sea level at pre-monsoon and −1 to 32 m above mean sea level at post-monsoon (Fig. 5). The
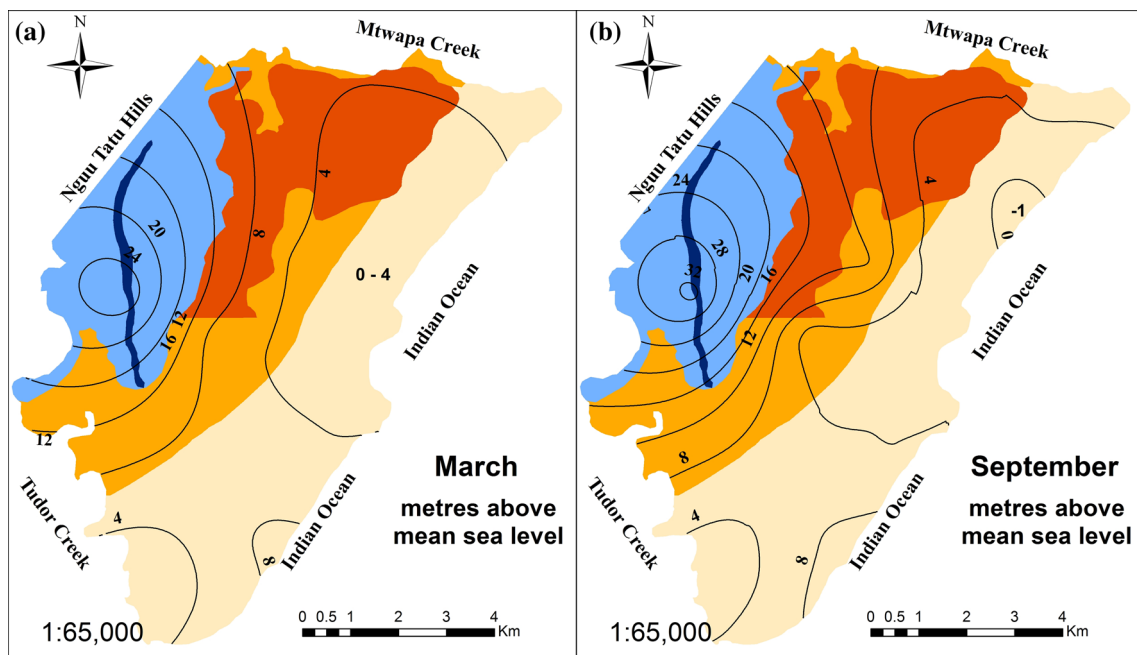
Fig. 5 Hydrogeological Map of Mombasa North Coast showing the groundwater levels at pre- and post-monsoon

groundwater table is generally shallow and supports the previous study by Munga et al. (2006). The contour maps for the NaCl, EC and TDS distributions for the pre-monsoon, rainy season and post-monsoon were all created to represent the hydrogeological condition of the study area.

The spatial distributions of the EC and TDS were somewhat similar (Figs. 6 and 7), indicating a strong relationship between their concentrations. The EC and TDS both showed a wider distribution of high concentrations (>1000 mg/l) in pre-monsoon than post-monsoon, especially towards the north-east and western parts of the study area which are in close proximity to the Ocean and creeks, respectively (Figs. 6 and 7). However, different dynamics were observed in the rainy season (June). Here, EC and TDS concentrations were below 1000 μS/cm and 500 mg/l, respectively, in large portions of the study area during the rainy season, with their concentrations increasing towards the Ocean (Figs. 6 and 7). It is likely that as the aquifer receives natural recharge from rainfall, it lowers the concentration of these parameters in groundwater. Also, higher groundwater flow during the rainy season as a result of rainfall recharge may tend to increase the hydraulic pressure of freshwater needed to shift the fresh/salt water wedge towards the sea (Wiest 1998). The peak monthly rainfall in the coast of Mombasa is experienced in the month of May averaging 238 mm, while April and June averages 159 and 88 mm, respectively (Climatemps 2015). Hence, a cumulative rainfall of almost 500 mm was experienced in the 3-month period between March (pre-monsoon) and the June data collection phase. As a

developing city, with a high aquifer recharge rate of 18–20% of the rainfall (Munga et al. 2004), the high rainfall recharge invariably contributed to the skewness of high EC and TDS concentrations towards the shore. The NaCl concentration which is a direct reflection of salinity showed a similar spatial trend with the EC and TDS (Fig. 8) signifying a strong relationship between the groundwater salinity and high values of EC and TDS in the aquifer. Figures 6, 7 and 8 show the spatial contours of the concentrations of the EC, TDS and NaCl concentrations, respectively.

Conclusions

Major groundwater parameters such as pH, EC, TDS, cations Na^+, K^+, Mg^{2+}, Ca^{2+} and anions Cl^-, HCO_3^-, SO_4^{2-} were analysed using statistical and spatial tools to understand the hydrogeochemical characteristics of the coastal aquifer of Mombasa North Coast. The groundwater pH was observed to be slightly alkaline with values ranging mostly between 7 and 8 although mildly acidic values may be experienced during the rainy season. This may be due to the rainfall recharge which is slightly acidic in nature. However, the pH values of over 90% of the samples fall within the Kenya drinking water limit (6.5–8.5) and 57% of the samples have pH values within WHO drinking water limit (7.5–8.5). Over 94% of EC and TDS values of the water samples obtained exceeded WHO drinking water limits of 750 μS/cm and 500 mg/l, respectively. However, only 43% of the water samples exceeded TDS
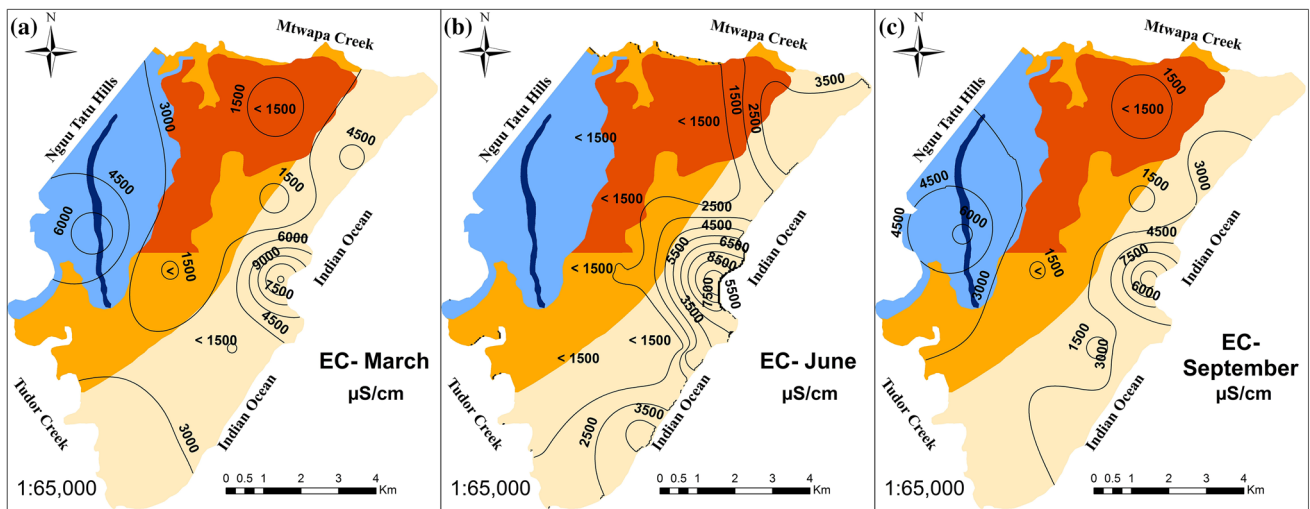
Fig. 6 *Contour lines* showing the spatial variation of EC values in the aquifer at **a** pre-monsoon, **b** rainy season and **c** post-monsoon
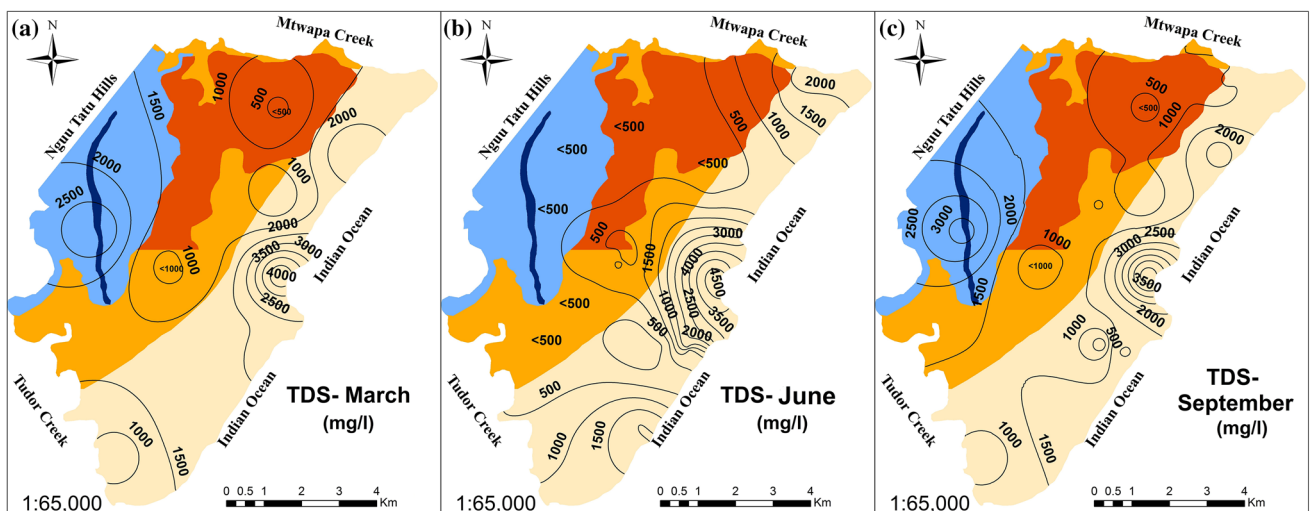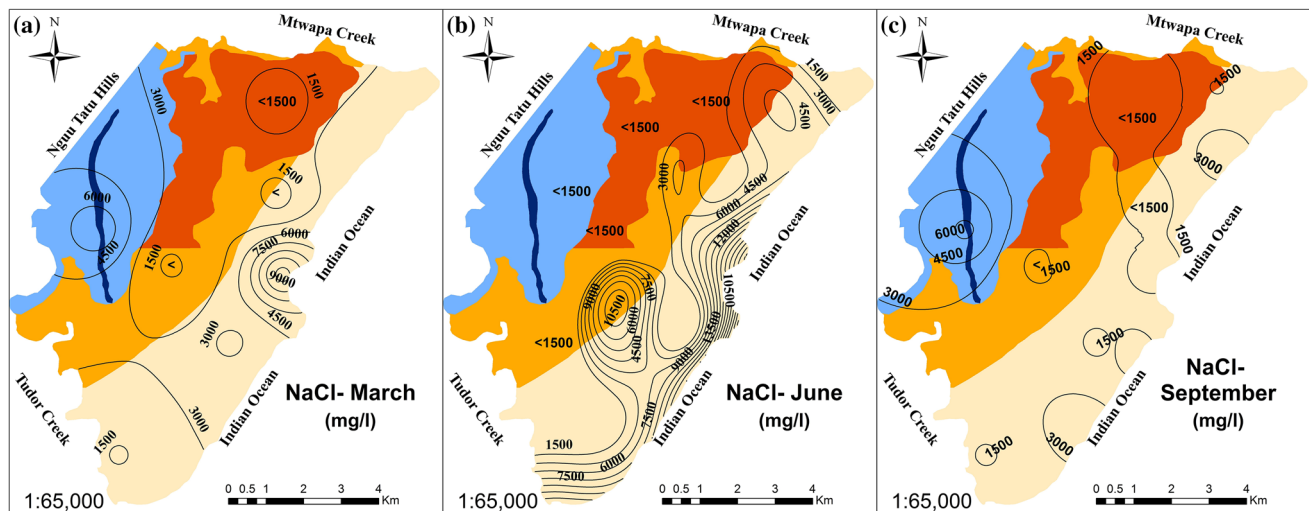

Fig. 7 *Contour lines* showing the spatial variation of TDS concentrations in the aquifer at **a** pre-monsoon, **b** rainy season and **c** post-monsoon

concentrations of 1500 mg/l, the limit set by Kenya drinking water guidelines. The highest values of EC and TDS were recorded at pre-monsoon (March)—10,585 µS/cm and 5281 mg/l, respectively. The EC classifications of the groundwater into fresh, brackish and saline waters suggest that higher groundwater salinity is experienced during the dry seasons. A near-perfect correlation was observed between EC and TDS values of the water samples. Seven parameters EC, TDS, Na^+, K^+, Mg^{2+}, Cl^- and SO_4^{2-} were observed to have strong correlations and hence have high impacts on the groundwater chemistry and have a tendency to follow similar trends. The Piper plots reveal the groundwater as Na–Cl waters and of the marine and deep ancient type. Further PCA and SMI statistical analysis reveals that the main contributor to the groundwater chemistry is seawater interaction, and to lesser extents are: complex natural processes, mineral dissolutions in the

aquifer formation and rainwater percolation. The water table levels in the study area are quite shallow with observed values of 0.90–29.89 m above mean sea level (msl) at pre-monsoon, −0.95 to 26.86 m and −0.84 to 30.08 m above msl in the rainy season and post-monsoon, respectively. The spatial variation maps of EC, TDS and NaCl show somewhat similar trends for both the pre-monsoon and post-monsoon, howbeit, relatively lower concentrations were observed in the latter. Close observation of the spatial maps for the rainy season shows that high concentrations of EC, TDS and NaCl were skewed towards the Ocean while the concentrations decreased with increasing distance to the Ocean. This implies that groundwater recharge from rainfall tended to facilitate the reduction of these concentrations inland. The constant interaction between the Ocean and the aquifer portion in close proximity to the Ocean might have accounted for the

Fig. 8 *Contour lines* showing the spatial variation of NaCl concentrations in the aquifer at **a** pre-monsoon, **b** rainy season and **c** post-monsoon

high concentrations of the EC, TDS and NaCl. The seasons affect the groundwater chemistry, and groundwater recharge from rainfall tends to slightly lower the values of EC, TDS and NaCl in the aquifer in the rainy season. The general high salinity observed in the groundwater renders the water unfit for direct drinking in many parts of the aquifer, but useful for domestic use. Finally, this study shows that a robust understanding of the hydrochemical characteristics of an aquifer can be obtained by combining the application of statistical and geospatial tools in groundwater studies.

References

Abdi H, Williams L (2010) Principal component analysis. Wiley Interdisciplinary Reviews: Computational Statistics 2(4):433–459. doi:10.1002/wics.101

Abuodha PA (2003) Geomorphology of the Kenyan coast: Not as a result of sea level change alone. Buletim Geologico no. 43 Mozambique. I - 8

Adams S, Titus R, Pietersen K, Tredoux G, Harris C (2001) Hydrochemical characteristics of aquifers near Sutherland in the western Karoo, South Africa. J Hydrol (Amst): 91–103. doi:10.1016/s0022-1694(00)00370-x

Adnan S, Iqbal J (2014) Spatial Analysis of the Groundwater Quality in the Peshawar District, Pakistan. Procedia Engineering 70:14–22. doi:10.1016/j.proeng.2014.02.003

Al-Ahmadi M, Subyani A (2010) Multivariate Statistical Analysis of Groundwater Quality in Wadi Ranyah, Saudi Arabia. Journal of King Abdulaziz University-Earth Sciences 21(2):29–46. doi:10.4197/ear.21-2.2

APHA (1995) Standard methods for the examination of water and waste water, 17th edn. American Public Health Association, Washington

Bakari SS, Aagaard P, Vogt RD, Ruden F, Johansen I, Vuai SA (2011) Delineation of groundwater provenance in a coastal aquifer using statistical and isotopic methods, southeast Tanzania. Environ Earth Sci 66(3):889–902. doi:10.1007/s12665-011-1299-y

Balathandayutham K, Mayilswami C, Tamilmani D (2017) Assessment of Groundwater Quality using GIS: A Case study of Walayar Watershed, Parambikulam-Aliyar-Palar Basin, Tamilnadu, India. Current World Environment, 10(2), 602-609. doi; http://dx.doi.org/10.12944/cwe.10.2.25

Banoeng-Yakubo B, Yidana SM, Nti E (2009) Hydrochemical analysis of groundwater using multivariate statistical methods—the Volta region. Ghana. KSCE J CIV ENG 13(1):55–63. doi:10.1007/s12205-009-0055-2

Barasa M, Crane E, Upton K, Ó Dochartaigh BÉ (2016) Africa Groundwater Atlas: Hydrogeology of Kenya. British Geological Survey. http://earthwise.bgs.ac.uk/index.php/Hydrogeology_of_Kenya Accessed 23 May 2017

Belkhiri L, Mouni L (2013) Geochemical modeling of groundwater in the El Eulma area, Algeria. Desalin Water Treat J 51(7–9):1468–1476. doi:10.1080/19443994.2012.699350

Beres M, Haeni FP (1991) Application of ground-penetrating-radar methods in Hydrogeologie studies. Gr Water 29(3):375–386. doi:10.1111/j.1745-6584.1991.tb00528.x

Brown CH (1998) Applied multivariate statistics in geohydrology and related sciences. Springer, Berlin

Caswell PV (2007) Geology of the kilifi-mazeras area (Report No 34, pp. 1–54), Reprinted (2007) Kenya, ministry of mining. Geology Department, Nairobi

Climatemps (2015) *Mombasa climate Mombasa temperatures Mombasa weather averages*. http://www.mombasa.climatemps.com/. Accessed 24 July 2016

Durgadevagi S, Annadurai R, Meenu M (2016) Spatial and temporal mapping of groundwater quality using GIS based water quality

index (A case study of IPCOT-Perundurai, erode. Indian J Sci Technol, Tamil Nadu. doi:10.17485/ijst/2016/v9i23/91484

GOK (1989) National population and housing census. Vol 1. Ministry of Planning and National Development, Central Bureau of Statistics, Nairobi

GOK (1999) National population and housing census. Vol 1. Ministry of Planning and National Development, Central Bureau of Statistics, Kenya

Goodchild M, Haining R (2004) GIS and spatial data analysis: converging perspectives. Pap Reg Sci 83(1):363–385. doi:10.1007/s10110-003-0190-y

Güler C, Thyne GD, McCray JE, Turner KA (2002) Evaluation of graphical and multivariate statistical methods for classification of water chemistry data. Hydrogeol J 10(4):455–474

Gulevich O, Volkomirskaya L (2015) Location of groundwater and distant detection of water pollution with use of GROT 12 Superpowerful Monopulse ground-penetrating radar. JWRHE 4(2):211–223. doi:10.5963/jwrhe0402012

Idowu TE, Nyadawa M, K'Orowe MO (2016) Seawater intrusion vulnerability assessment of a coastal aquifer: north Coast of Mombasa, Kenya as a case study. Int J Eng Res Appl 6(8–3):37–45

Igrac (2017) Transboundary aquifers of the world map. Ggis.un-igrac.org. https://ggis.un-igrac.org/ggis-viewer/viewer/tbamap/public/default. Accessed 23 May 2017

Jothivenkatachalam K, Nithya A, Chandra Mohan S (2010) Correlation analysis of drinking water quality in and around Perur block of Coimbatore District, Tamil Nadu, India. Ras J Chem 3(4):649–654

Kaiser H (1960) The application of electronic computers to factor analysis. Educ Psychol Meas 20(1):141–151. doi:10.1177/001316446002000116

Kallioras A, Pliakas FK, Schuth C, Rausch R (2013) Methods to countermeasure the intrusion of seawater into coastal aquifer systems. In: Sanghi R (ed) Sharma SK. Springer, Wastewater Reuse and Management. doi:10.1007/978-94-007-4942-9_17

Karmegam U, Chidambaram S, Prasanna MV, Sasidhar P, Manikandan S, Johnsonbabu G, Anandhan P (2011) A study on the mixing proportion in groundwater samples by using piper diagram and Phreeqc model. Chin J Geochem 30(4):490–495. doi:10.1007/s11631-011-0533-3

Kenya WASREB (2008) Water services regulatory board Drinking water quality and effluent monitoring guideline. http://www.waterfund.go.ke/toolkit/Downloads/2.%20Drinking%20Water%20Guidelines.pdf. Accessed 20 Sep 2016

KNBS (2010) 2009 Kenya population and housing census, Population distribution by political units, vol.1B, KNBS

Kumar CP (2006) Management of Groundwater in Salt Water Ingress Coastal Aquifers. In: Ghosh NC, Sharma KD (eds) Groundwater modelling and management. Capital Publishing Company, New Delhi, pp 540–560

Mondal N, Singh V, Saxena V, Prasad R (2008) Improvement of groundwater quality due to fresh water ingress in Potharlanka Island, Krishna delta, India. Environ Geol 55(3):595–603. doi:10.1007/s00254-007-1010-5

Mondal NC, Singh VP, Singh VS, Saxena V (2010) Determining the interaction between groundwater and saline water through groundwater major ions chemistry. J Hydrol 388(1–2):100–111. doi:10.1016/j.jhydrol.2010.04.032

Mondal NC, Singh VP, Singh S, Singh V (2011a) Hydrochemical characteristic of coastal aquifer from Tuticorin, Tamil Nadu, India. Environ Monit Assess 175(1–4):531–550. doi:10.1007/s10661-010-1549-6

Mondal NC, Singh VS, Saxena VK, Singh VP (2011b) Assessment of seawater impact using major hydrochemical ions: a case study from Sadras, Tamilnadu., India. Environ Monit Assess 177(1–4):315–335. doi:10.1007/s10661-010-1636-8

Moujabber ME, Samra BB, Darwish T, Atallah T (2006) Comparison of different indicators for groundwater contamination by seawater intrusion on the Lebanese coast. Water Resour Manag 20(2):161–180. doi:10.1007/s11269-006-7376-4

Mtoni Y, Mjemah IC, Msindai K, Van Camp M, Walraevens K (2012) Saltwater intrusion in the quaternary aquifer of the Dar es Salaam region, Tanzania. Geol Belg 15(1–2):16–25

Mtoni Y, Mjemah IC, Bakundukize C, Van Camp M, Martens K, Walraevens K (2013) Saltwater intrusion and nitrate pollution in the coastal aquifer of Dar es Salaam, Tanzania. Environ Earth Sci 70(3):1091–1111. doi:10.1007/s12665-012-2197-7

Munga D, Kitheka JU, Mwangi S, Ong'anda H, Mwaguni SM, Massa HS, Mwashote BM, Muthuka MM, Chidagaya SJ, Mdoe F, Opello G (2004) Pollution and vulnerability of water supply aquifers in Mombasa Kenya: interim progress report (p 29). Mombasa, Kenya: Kenya Marine Fisheries and Research Institute. http://www.oceandocs.org/bitstream/handle/1834/6972/ktf0056.pdf?sequence=1&isAllowed=y. Accessed 24 May 2017

Munga D, Mwangi S, Ong'anda H, Kitheka JU, Mwaguni SM, Mdoe F, Opello G (2006) Vulnerability and pollution of groundwater in Kisauni, Mombasa, Kenya. In: Youngxin X, Brent U (eds) Groundwater pollution in Africa. Taylor and Francis (Balkema), The Netherlands

Musa OK, Kudamnya EA, Omali AO, Akuh TI (2014) Physico-chemical characteristics of surface and groundwater in Obajana and its environs in Kogi state, central Nigeria. Afr J Environ Sci Technol 8(9):521–531. doi:10.5897/ajest2014.1708

National Environment Secretariat (1985) Mombasa district environmental assessment report (pp 5–7). Nairobi: ministry of environment and natural resourses. http://pdf.usaid.gov/pdf_docs/PNAAU556.pdf. Accessed 05 Mar 2017

Okiongbo KS, Douglas RK (2014) Evaluation of major factors influencing the geochemistry of groundwater using graphical and multivariate statistical methods in Yenagoa city, southern Nigeria. Appl water sci 5(1):27–37. doi:10.1007/s13201-014-0166-x

Olayinka A, Amidu S, Oladunioye M (2004) Use of electromagnetic profiling and resistivity sounding for groundwater exploration in the crystalline basement area of Igbeti, Southwestern Nigeria. Global J Geol Sci 2(2):243–253. doi:10.4314/gjgs.v2i2.18701

Peeters L (2013) A background color scheme for piper plots to spatially visualize Hydrochemical patterns. Groundwater 52(1):2–6. doi:10.1111/gwat.12118

Piper AM (1953) A graphic procedure in the geochemical interpretation of water analysis. USGS, Washington. OCLC 37707555. ASIN B0007HRZ36

Rai NS (2004) Role of mathematical modeling in groundwater resources management. Sri Vinayaka Enterprises, Hyderabad, pp 434–445

Ratner B (2009) The correlation coefficient: its values range between +1/− 1, or do they? J Target Meas Analy Mark 17(2):139–142. doi:10.1057/jt.2009.5

Ravikumar P, Somashekar R (2015) Principal component analysis and hydrochemical facies characterization to evaluate groundwater quality in Varahi river basin, Karnataka state, India. Appl Water Sci 7(2):745–755. doi:10.1007/s13201-015-0287-x

Sappa G, Ergul S, Ferranti F, Sweya LN, Luciani G (2015) Effects of seasonal change and seawater intrusion on water quality for drinking and irrigation purposes, in coastal aquifers of Dar es Salaam, Tanzania. J Afr Earth Sci 105:64–84. doi:10.1016/j.jafrearsci.2015.02.007

Schwartz M (2006) Encyclopedia of coastal science, 1st edn. Springer, New York, p 358

Schwartz A, Gupta S, Patil R (2005) Statistical analyses of coastal water quality for a port and harbour region in India. Environ Monit Assess 102(1–3):179–200. doi:10.1007/s10661-005-6021-7

Sheikhy Narany T, Ramli MF, Aris AZ, Sulaiman WN, Juahir H, Fakharian K (2014) Identification of the Hydrogeochemical processes in groundwater using classic integrated Geochemical methods and Geostatistical techniques, in Amol-Babol plain, Iran. Sci World J 2014:1–15. doi:10.1155/2014/419058

Sindhu G, Ashith M, Jairaj PG, Raghunath R (2012) Modelling of coastal aquifers of Trivandrum. Proc Eng 38:3434–3448. doi:10.1016/j.proeng.2012.06.397

Somay MA, Gemici Ü (2008) Assessment of the salinization process at the coastal area with hydrogeochemical tools and geographical information systems (GIS): selçuk plain, Izmir, turkey. Water Air Soil Pollut 201(1–4):55–74. doi:10.1007/s11270-008-9927-1

Volker RE, Zhang Q, Lockington DA (2002) Numerical modelling of contaminant transport in coastal aquifers. Math Comput Simul 59(1–3):35–44. doi:10.1016/s0378-4754(01)00391-3

WHO (2011). Guideline of drinking quality. Fourth Edition WHO Press, World Health Organization, 20 Avenue Appia, 1211 Geneva 27, Switzerland http://www.who.int. Assessed 24 Apr 2016

Wiest RJM (1998) Ghyben–Herzberg theory. In: Herschy RW, Fairbridge RW (eds), Encyclopaedia of hydrology and lakes. pp 340–341. doi:10.1007/1-4020-4497-6_104

Xuedi Z, Jianhua W, Baode (2011) Application of principal component analysis in groundwater quality assessment. In: 2011 international symposium on water resource and environmental protection. http://dx.doi.org/10.1109/iswrep.2011.5893671

Yan S, Chen MS, Shi XX (2009) Transient electromagnetic sounding using a 5 m square loop. Explor Geophys 40(2):193. doi:10.1071/eg08122

Ziani D, Boudoukha A, Boumazbeur A, Benaabidate L, Fehdi C (2016) Investigation of groundwater hydrochemical characteristics using the multivariate statistical analysis in Ain Djacer area, eastern Algeria. Desalin Water Treat 57(56):26993–27002. doi:10.1080/19443994.2016.1180474